Seismic response of bridges with cellular foundations built in soft clay

Juan M. Mayoral, Miguel P. Romo & Francisco A. Flores
Institute of Engineering, UNAM, Mexico City, Mexico

ABSTRACT
A new foundation system based on structural cells has been used for supporting the columns of the elevated section of the 12th Metro Line, in Mexico City. This study consists on a numerical simulation employing a three-dimensional finite element model developed with the program SASSI2000, of one of the critical supports located in the so-called Lake zone, known by its difficult subsoil conditions. Clays in this region present low shear strength and high compressibility. The system response was computed for a typical seismic scenario, such as that prevailing at the zone, which assumes a potential M_w=8.2 seismic event. The cellular foundation is comprised of a rigid slab structurally tied to perimeter concrete walls, also structurally connected to each other. The computed upper deck acceleration is less than a half of that obtained directly from the recommended response spectra compiled in the Mexico City building code.

RESUMEN
Un nuevo sistema de cimentación basado en celdas estructuradas va a ser empleado para soportar las columnas del tramo elevado de la Línea 12 del Metro de la Ciudad de México. El estudio aquí presentado, consiste en la simulación numérica, usando un modelo tridimensional de elementos finitos desarrollado con el programa SASSI2000, de uno de los apoyos más críticos localizado en la denominada zona de Lago conocida por sus difíciles condiciones del subsuelo. Las arcillas en esta región presentan una baja resistencia al esfuerzo cortante y alta compresibilidad. La respuesta del sistema fue calculada para un escenario típico, como el que prevalece en la zona, asumiendo un evento sísmico de magnitud M_w = 8.2. La celda estructurada está conformada por una losa rígida conectada estructuralmente a muros perimetrales de concreto también conectados entre sí. La acceleración máxima calculada en la parte superior del tramo elevado es menor que la mitad de la obtenida directamente del espectro de diseño propuesto por el reglamento de construcciones de la Ciudad de México.

1 INTRODUCTION

A new 28.4 km long metro line is under construction in the southeast part of Mexico City, the so-called 12th Line. In particular, 13 km of this project will be elevated, and will cross two of the most difficult subsoil conditions in the city, the lake zone and the transition zone (Figure 1). A new foundation alternative (Romo *et al.*, 2010) based on a skirted type foundation, consisting on a mat structurally tied to peripheral walls was used to support the columns of the elevated section (Figure 2a). This work presents the seismic performance evaluation of one of the most critical supports, hereafter referred as cl-34, which is located in the typical soft clay deposits found at the city. The seismic soil-structure interaction analyses were conducted using 3-D finite element models, considering a seismic environment characterized by a major seismic event, with moment magnitude, M_w, of 8.2. The response of the structure was obtained in terms of accelerations, displacements and response spectra. Transfer functions between free field and both foundation and structure were also computed. The high stiffness of both the column and the cellular foundation reduce the maximum accelerations obtained in the upper deck.

2 SUPPORT ANALYZED

Figure 2 shows support cl-34 in elevation and plan view. Figure 2c depicts a longitudinal view of the elevated section. This consists of an upper deck resting on top of 30 m long beams, which are, in turn, supported by columns. Both beams and columns are pres-stress and made of high strength concrete. The columns have a hollow transversal section, and are structurally connected to the cellular foundation. The upper part of this foundation consists of a rigid square concrete mat 6.5 x 6.5 m^2, with 1.7 m of thickness. This slab is rigidly attached to perimeter structural concrete walls 0.60 m thick. The embedment depth of this foundation is 15 m (Figure 2a).

3 SUBSOIL CONDITIONS

To characterize the geotechnical subsoil conditions found at the site, one cone penetration test, CPT, and one standard penetration test, SPT, combined with selective undisturbed sampling were conducted. The studied site is mostly comprised by a very soft to medium clay deposits interbedded with thin sand lenses. Figure 3 shows the soil profile, the variation of tip penetration resistance with depth, SPT values, and rock core recovery percentage. Based on the field investigation and laboratory testing results, it was found that the soil profile is comprised by a sandy silt layer 3 m thick. Underlying this stratum, there is a soft to medium 25 m clay layer interbedded with silty sand lenses. Within this layer, from 3 to 7 m of depth, there is a high plasticity clay layer. At 6.5 m, water content, ω_n (%), is 400 %, liquid limit, ω_L(%), is 450 % and plasticity index, *PI*, is 172 %. Below 7 m and up to 21 m, ω_n (%), varies from 50 to 200 % and the undrained shear

strength, s_u, goes from 21 kPa to 40 kPa. From 21 m to 28 m of depth, there is a low plasticity sandy clay layer, exhibiting a ω (%) of about 30. The preconsolidation pressure, σ'_p, is 10 kPa for both 6.5 m and 9.5 m of depth, and for 14.5 m, σ'_p, is 196 kPa. The coefficient of volumetric compressibility, m_v, ranges from 0.162 cm^2/kg to 0.047 cm^2/kg.

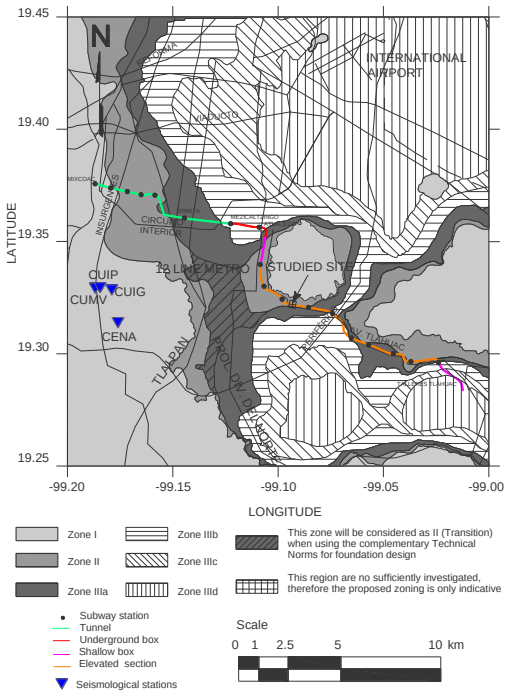

Figure 1. Project location and geotechnical zoning in Mexico City

3.1 Shear wave velocity distribution

Due to the lack of shear wave velocity, V_s, field measurements, these were estimated with empirical correlations proposed by several authors. Equation 1 recommended by Seed et al. (1981) was used to estimate V_s for sands.

$$V_s = 61\sqrt{N_{1(60)}} \qquad [1]$$

Where: V_s is the shear wave velocity in m/s, $N_{1(60)}$ is the number of blows counts corrected by energy and overburden pressure, expressed in terms of the confining stress, σ', in Eq. 2.

$$N_{1(60)} = N_{60}\sqrt{\frac{10}{\sigma'}} \qquad [2]$$

The shear wave velocity distribution with depth for clays was estimated using the expression proposed by Ovando and Romo (1991), in terms of the tip penetration resistance, q_c, measured with CPT.

$$V_s = \eta\sqrt{\frac{q_c}{N_{kh}\gamma_s}} \qquad [3]$$

Where: V_s is the shear wave velocity in m/s, q_c is the tip cone penetration resistance in t/m^2; γ_s is the unit weight of the soil, in t/m^3; N_{kh} and η are parameters that depend on the soil type. For this study, N_{kh}=9.9 and η=26.4 (Ovando and Romo, 1991).

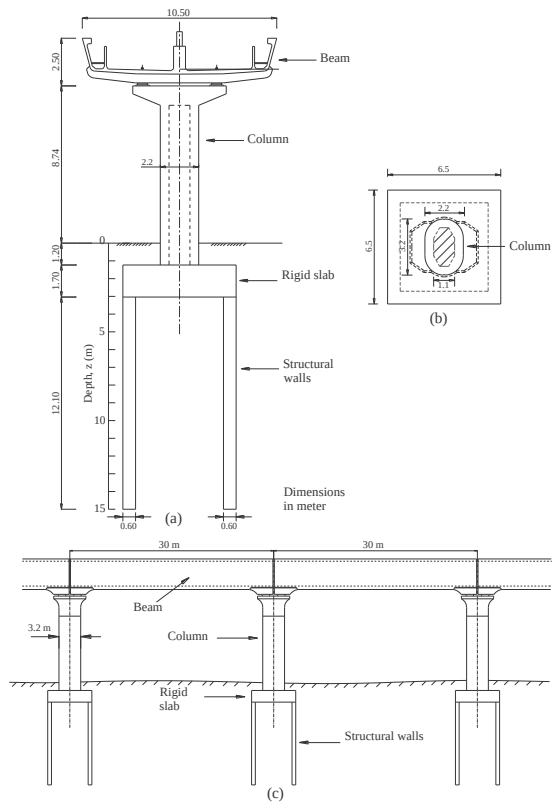

Figure 2.Support analyzed: (a) elevation, (b) plan view and (c) longitudinal view of the elevated section

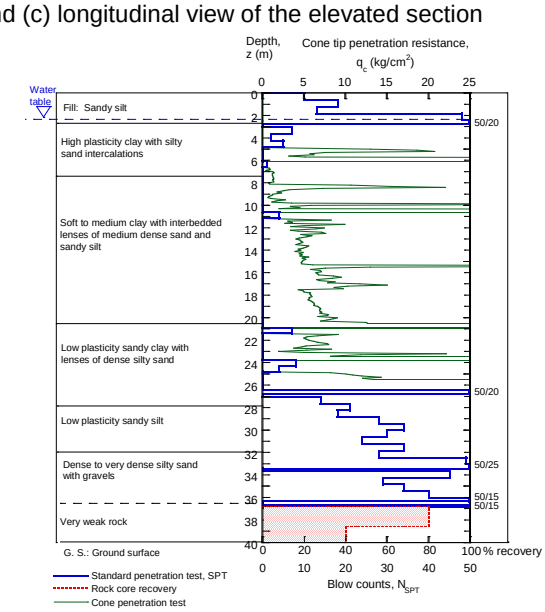

Figure 3. Subsurface conditions at the studied site

Figure 4 presents the shear wave velocity profile estimated with expressions 1 to 3. The solid line is the representative average of V_s considered for analysis. The

shear wave velocity of clayey soils ranges from 40 to 120m/s and for granular materials goes from 230 and 430 m/s.

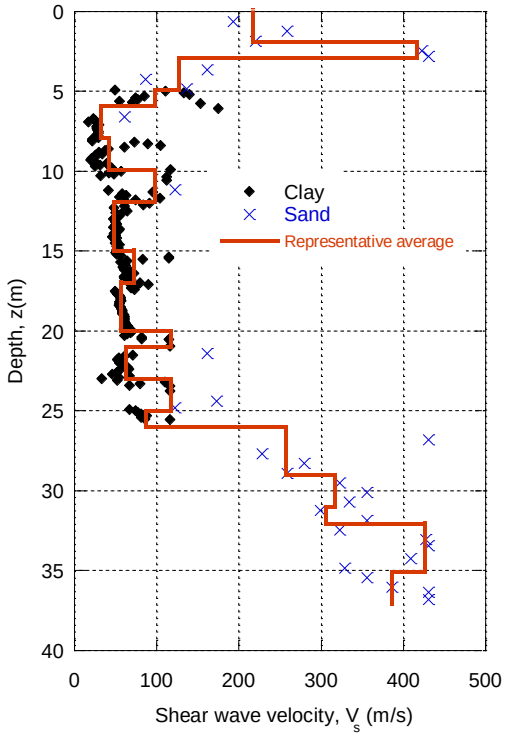

Figure 4. Shear wave velocity profile

3.2 Normalized modulus degradation and damping curves

For clays:
Due to the limited experimental information available, the normalized shear modulus degradation and damping curves, recommended by Vucetic and Dobry (1991), as a function of plasticity index, were used for the clays found at the site (Figure 5). These were compared against the experimental data obtained from two sets of results of resonant column and triaxial tests. Figure 5 shows these results (Romo *et al*., 2010), and previous experimental results gathered by Enriquez et al. (2008). Vucetic and Dobry (1991) curves seem to provide a good match to the measured response.

For sands:
Curves proposed by Seed and Idriss (1970) were used for sands (Figure 6). G/G_{max}–γ and λ–γ curves presented in Figures 5 and 6 have been successfully used in one-dimensional wave propagation analyses to predict the seismic response during the 1985 Michoacan earthquake (e.g. Romo y Seed, 1986; Romo, 1995; Mayoral et al., 2008).

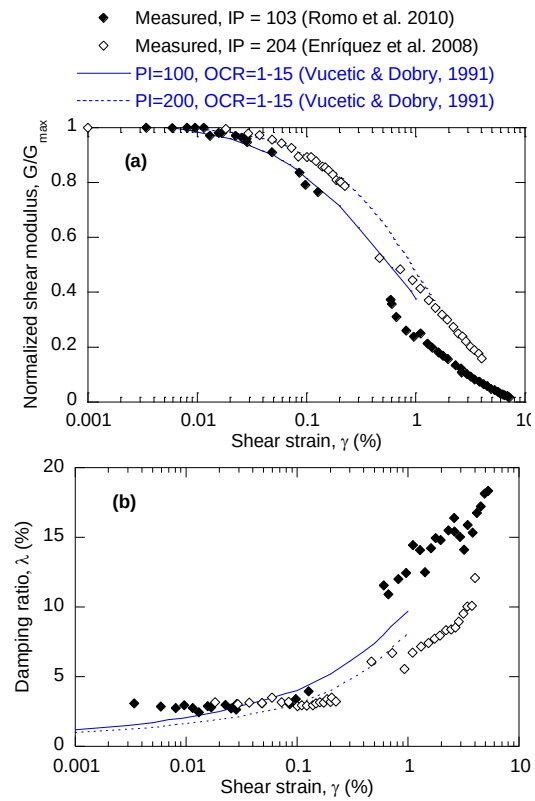

Figure 5. Comparison of (a) G/G_{max}-γ and (b) λ-γ curves reported in technical literature with experimental results.

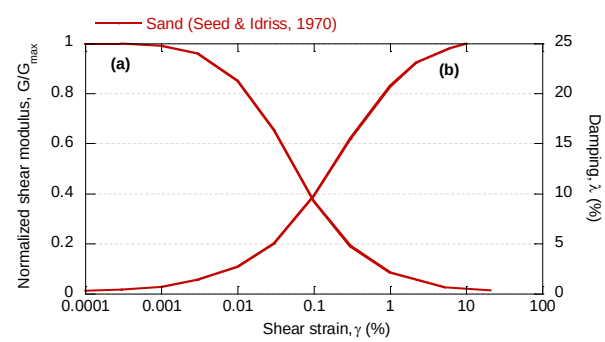

Figure 6. Normalized shear modulus (a) and damping curves for sands (b)

3.3 Seismic environment

The seismic environment was defined using the historical seismicity recorded at the site. Initially, a search of the seismological stations, located on rock or firm soils, situated near the project site was conducted. These were identified as CUIP, CUMV, CUIG and CENA (Figure 1), which are located in average at 10 km away from the analyzed support. Only the seismic events with M_w larger than 6.5, reported in the Mexican Strong Earthquake Data Base (BMSF, 1996), were considered. Response spectra of both horizontal components of these events were obtained for the four stations. Each response spectrum was normalized with respect to its peak ground

acceleration, PGA. These were, then, scaled to a PGA of 0.085 g. This acceleration corresponds to a magnitude earthquake M_w=8.2, obtained with the attenuation relationship proposed by Crouse (1991), for an event located at about 330 km of the studied site. The response spectrum obtained from the mean, μ, plus one standard deviation, σ, values, was used for this study. Both frequency content and amplitude of the response spectrum compiled in the Mexico City building code (RCDF, 2004) for the hill zone, are well covered by the $\mu + \sigma$, spectrum. The acceleration time history shown in Figure 7b was obtained from a time domain spectral matching of the design response spectrum obtained from this study, using the methodology proposed by Lilhanand and Tseng (1998) as modified by Abrahamson (1993).

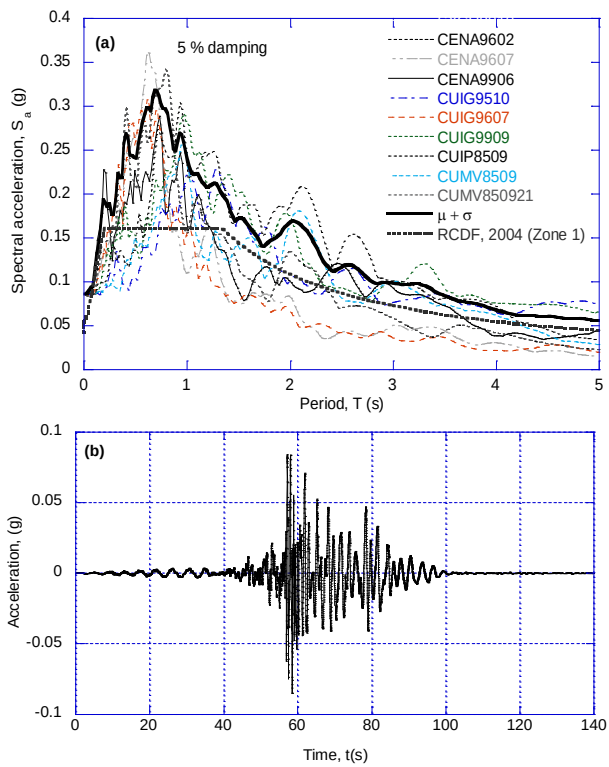

Figure 7. (a) Normalized response spectra and (b) synthetic acceleration time history

4 SOIL-STRUCTURE INTERACTION

4.1 Numerical model

To study the seismic response of cellular foundations, a finite element model of support cl-34 was developed with the program SASSI 2000 (Lysmer et al., 2000), using the flexible volume method. The flexible volume method is formulated in the frequency domain, through the complex response method and finite element technique as described by Lysmer (1978). The soil-structure system was divided into the soil, the foundation and the structure. For the analyses, the structure was modeled with beam elements and lumped masses. Both the foundation and the near field soil were simulated with three-dimensional solid finite elements (Figure 8 and Figure 9).

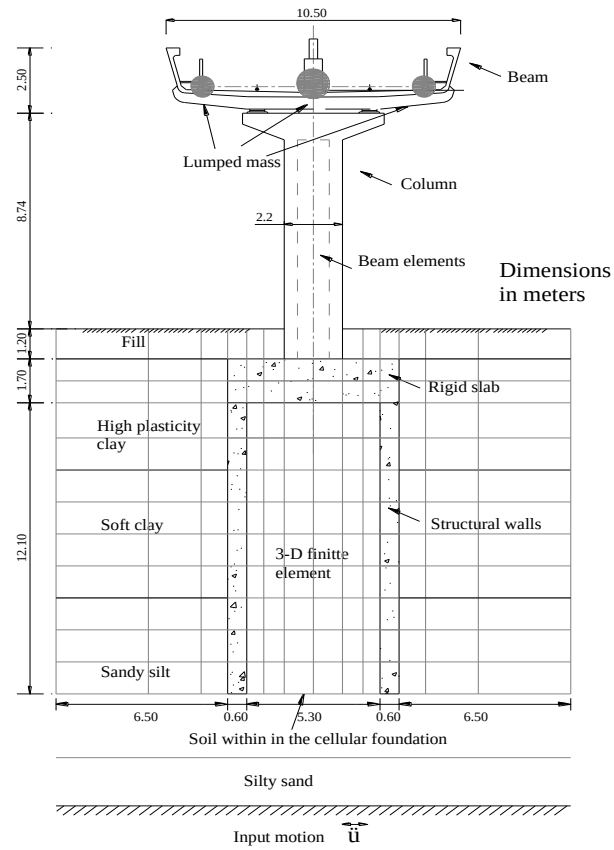

Figure 8. Schematic representation of foundation support

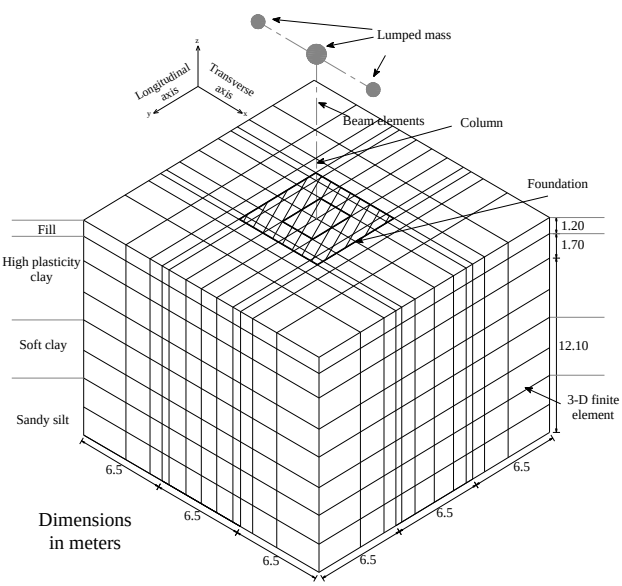

Figure 9. Finite element model for support cl-34

The soil was considered as axis-symmetric, and comprised by series of semi-infinite visco-elastic

horizontal layers with equivalent linear properties (i.e. shear stiffness and damping) resting on top of a visco-elastic half space. The soil-foundation–structure interaction occurs at all basement nodes. Absorbing transmitting boundaries were used at the edges of the models to simulate the free field conditions. Only transversal effects were studied.

4.1.1 Soil model

The soil within the cellular foundation was modeled with three-dimensional solid finite elements. The small strain shear stiffness (i.e. γ less than 10^{-4} %) of the soil was assumed for the elements found within the cellular foundation, considering that the ground movement is restricted by the cellular structure. Thus, a damping ratio of 3 % was deemed appropriated for these soil elements. Regarding to the near and far field soil, this was modeled with equivalent linear properties, which were obtained from a site response analysis conducted with the program SHAKE. Studies carried out by several researchers (Romo and Seed, 1986; Romo, 1995; Mayoral *et al*., 2008) have proven that using equivalent linear properties is enough to represent the soil-nonlinearities both in high plasticity clayey and sandy silts, at least for moderate to high level of shaking (M_w ranging from 6 to 8.2).

4.1.2 Substructure model

The cellular foundation was represented with three-dimensional solid finite elements (Figure 8). The structure damping was modeled using a Rayleigh type formulation. Table 1 shows the structural members properties.

Table 1. Strength concrete of structural elements.

Structural element	Unit weight, γ_m (kN/m3)	Young modulus, E (MPa)	Strength concrete f'_c (kPa)
Pre-cast columns and beam	24.5	30,000	60,000
Structural walls	23.5	25,600	35,000
Reinforced rigid slab	23.5	30,000	60,000

*Poisson ratio ν = 0.3
Damping ratio λ = 3 %

4.1.3 Superstructure model

The structure was simulated with lumped masses and beam elements (Figure 9). The total mass of the upper deck and beams was concentrated in three lumped masses to distribute the upper deck inertia, connected by rigid members to the beams elements that represent the columns, simulated with eleven beam elements (Figure 2). The column was made of high strength concrete with hollow transversal section. Table 1 shows the concrete properties.

4.2 Seismic response of the support analyzed

The seismic response of support cl-34 was computed at five vertical axes: in the near field, A1-A5 and B1-B-5, outside of the cellular foundation, C1-C5, and the soil inside it, D3-D5 and E3-E5. The control points shown in Figure 10 indicate the depths where response spectra were computed. These points are located at 0.0, 2.9 m, 8 m and 15 m.

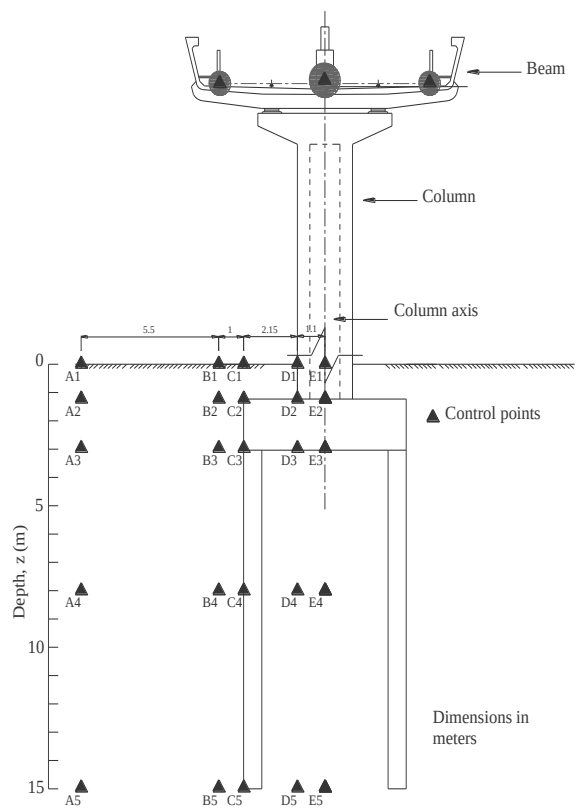

Figure 10. Control points location in the soil-foundation-structure system

Figure 11 shows the comparison at axis A through E of response spectra computed at different depths (i.e. ground surface, at 2.9 m, 8 m and 15 m). Important differences both in spectral amplitudes and frequency contents can be seen. Figure 12 shows the variation of the response spectra along Axis E, control points from E1 to E5, with respect to the free field, calculated at the ground surface. Important amplifications were observed in shallower points. The spectral accelerations at the bottom of the column are higher than those accelerations computed at free field for a period ranging from 1 to 1.6 s, whereas for periods going from 2 to 3 s, are lower.

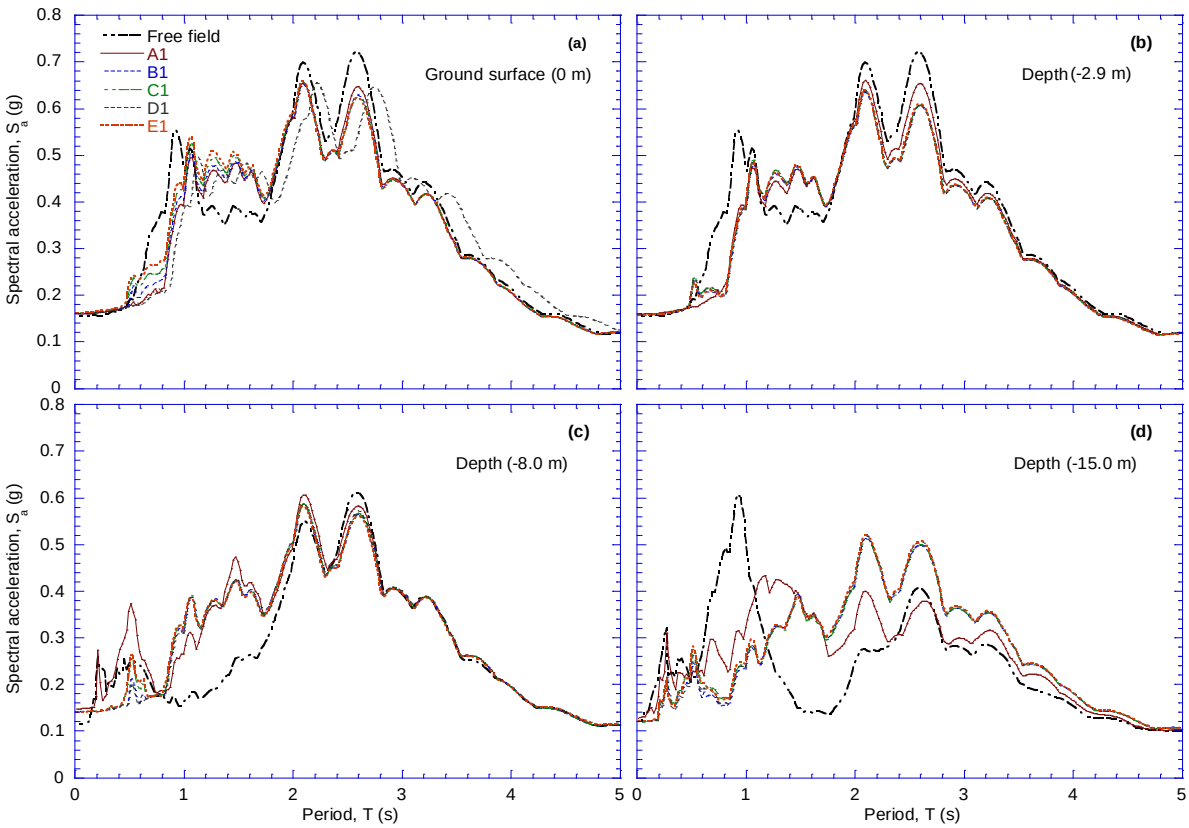

Figure 11. Response spectra calculated at several depths in axis A through E

At a soil-structure interaction period, T_{SEI}, of 2.6 s (f_{SEI} = 0.38 Hz) an attenuation of 10 % of the maximum spectral acceleration with respect to the free field response was observed. However, the actual response of the structure is controlled by the high stiffness of the column-foundation system, which reduces the computed acceleration to 0.162 g at the foundation (Figure 13b), and 0.166 g at the support beam (Figure 13c). These values are closed to the response obtained from the period computed for the structure, considering it on top of a rigid base (i.e 0.16 s (f = 6.25 Hz)). This fact leads to an important reduction of the accelerations generated at the upper deck, as can be noticed in the calculated acceleration times histories (Figure 13). Figure 13 also depicts the acceleration time histories obtained at free field, foundation and support beam. Figure 14 shows the corresponding displacements, overall are very similar to those computed at the upper deck. The maximum accelerations obtained at free field, cellular foundation and support beam are 0.157 g, 0.162 g y 0.166 g, respectively. From this study it is concluded that the response of the soil-foundation-structure system is controlled by the high stiffness of the foundation-column system. Both the maximum relative displacement, between the cellular foundation with respect to the support beam, and thus, the maximum distortion of the column, occurred at 83.20s. The maximum displacements computed at the free field, cellular foundation and support beam were 23.98 cm, 21.46 cm and 22.93 cm, respectively, at this time. The distortion generated between the foundation and support beam was obtained from the subtraction of the maximum displacements between both points, divided by the length column (L= 10.59 m). The maximum distortion was 0.00139.

Figure 14 shows the rotations of both the rigid slab and support beam. The maximum rotation of the rigid slab is 0.0032 rad (0.17º).

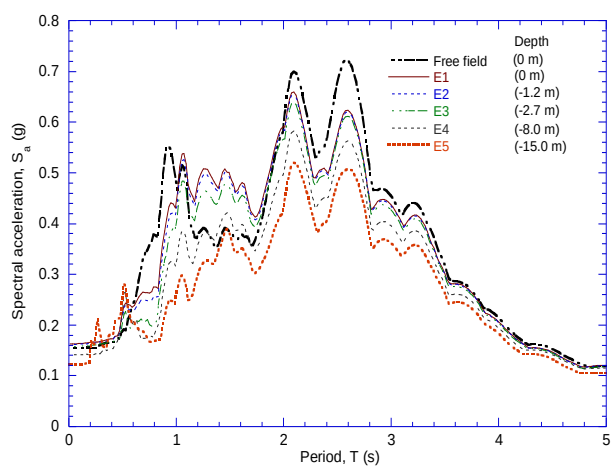

Figure 12. Response spectra calculated along axis E

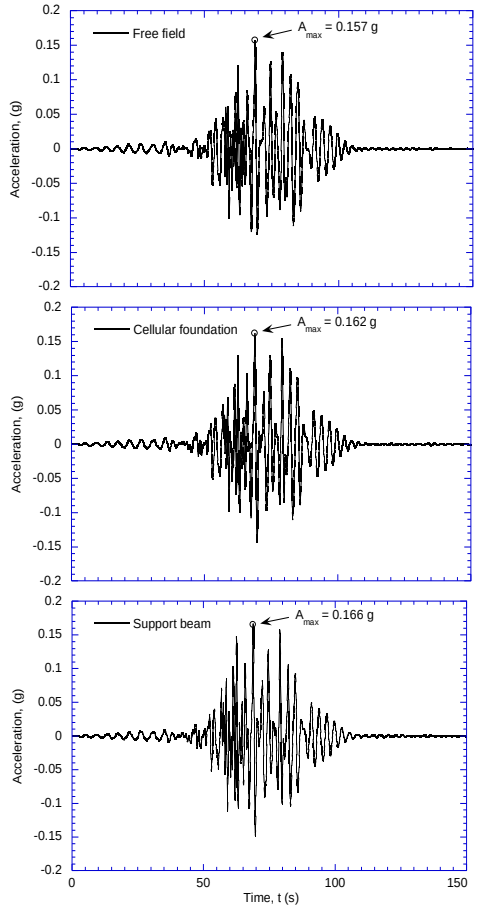

Figure 13. Acceleration time histories calculated at the (a) free field, (b) cellular foundation and (c) support beam

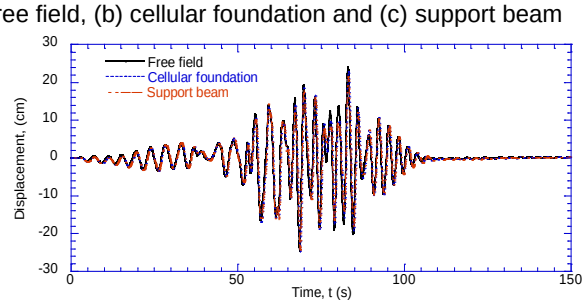

Figure 13. Displacement time histories calculated at the (a) free field, (b) cellular foundation and (c) support beam

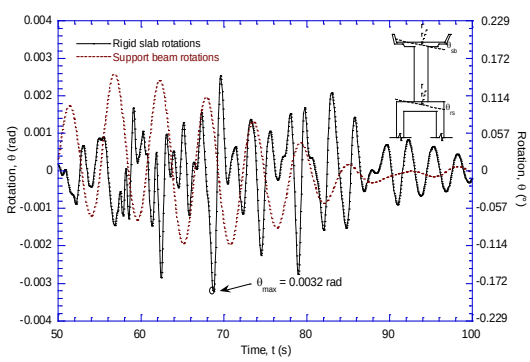

Figure 14. Rigid slab and support beam rotations

The point of rotation shifts back and for during the period of time the excitation is acting on the system. At the particular time associated to the larger movement (i.e. 68.75s), it is located at 9.67 m of depth and at 2.21 m with respect to the vertical axis column, as depicted in Figure 15. The foundation moves almost as a rigid body. The horizontal displacements of the soil at the five vertical axes previously defined are also included in this figure. For the maximum rotation, the horizontal relative displacement, between the top of the slab and the bottom of the structural concrete wall, is 0.045 m. Figure 16 shows the deformed shapes of the column at different times during the seismic event. The maximum displacement of the column was about 0.05 m at 68.75 s, which is consistent with the high stiffness of the foundation-structure system, and the column supporting the upper beam. According to the numerical study, the seismic performance of the soil-structure system is satisfactory for the design earthquake (M_w=8.2).

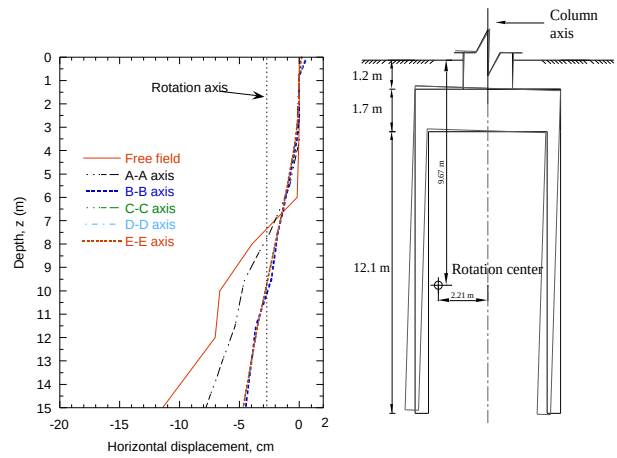

Figure 15. Movements of the cellular foundation and soil at time t = 68.75 s.

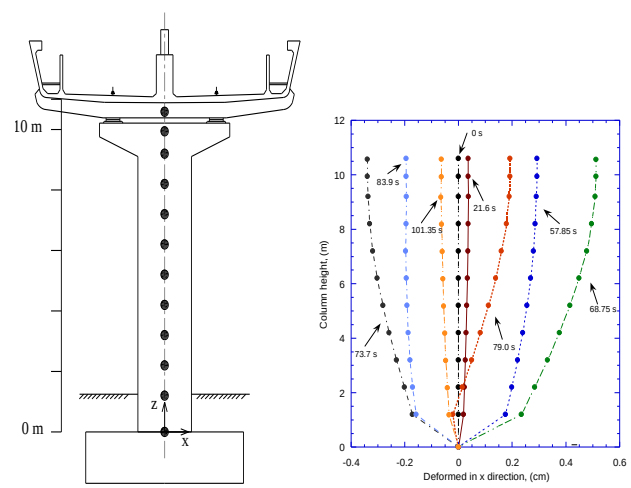

Figure 16. Deformed shape of the column at several times

5 CONCLUSIONS

A two tridimensional finite element model was developed to evaluate the seismic response of a cellular foundation, including soil-foundation-structure interaction effects. Due to the high stiffness of both the column and soil-foundation system, the seismic response was mostly at low periods. This effect reduces the maximum acceleration, and therefore seismic forces computed at the support beam (i.e. 0.17 g). This is in agreement with the small lateral displacements computed between the foundation and support beam, which are about 0.05 m. Rotations at the cellular foundation are about 0.0032 rad. The maximum acceleration computed in the support beam is lower than half of that recommended by the RCDF building code for period from 0.2 to 1.3 s. (i.e. 0.16 g).

REFERENCES

Abrahamson N. 1993. Non-stationary spectral matching program, unpublished.

BMSF, 1996. Base Mexicana de Datos de Sismos Fuertes. Actualización de los Catálogos de Estaciones a 1995 y Acelerogramas a 1994. *SMIS*, CD; 1996.

Crouse CB. 1991. Ground-motion attenuation equations for earthquakes on the Cascadia subduction zone. Earthquake Spectra, vol. 7, No. 2.

Enríquez O., Osorio L., Flores O. and Mayoral J. M. 2008. Determinación de las propiedades dinámicas de arcillas blandas de la zona noreste del ex Lago de Texcoco. *XXIV Reunión Nacional de Mecánica de Suelos SMMS*, Aguascalientes, Ags., noviembre 2008 pp 121-127

Lilhanand K. and Tseng W. S. 1988. Development and application of realistic earthquake time histories compatible with multiple damping response spectra, *Proceedings of the 9th World Conference on Earthquake Engineering*, Tokyo, Japan, Vol. II, pp 819-824.

Lysmer J. Analytical procedures in soil dynamics; *Report No. EERC 78/29*, University of California, Berkeley, December 1978

Lysmer J, Ostadan F, Tabatabaie M, Tajirian F, Vahdani S. SASSI, A System for Analysis of Soil-Structure Interaction; University of Berkeley, CA. 2000

Mayoral JM, Romo MP, Osorio L., 2008. Seismic parameters characterization at Texcoco lake, Mexico. *Soil Dynamics and Earthquake Engineering*; 28(7):507–521.

Ovando E. and Romo M. P. 1991. Estimación de la velocidad de ondas S en la arcilla de la ciudad de México con ensayos de cono, *Revista Sismodinámica*, 2, 107-123.

Romo M. P. 1995. Clay behavior, soil response and soil structure interaction studies in Mexico City. *Proceedings of the third International Conference on Recent Advances in Geotechnical Earthquake Engineering and Soil Dynamics*, vol. 2, San Louis Missouri, U.S.A.; 1039–1051.

Romo M. P. and Seed H. B. 1986. Analytical modeling of dynamic soil response in the Mexico earthquake of September 19, 1985, *Proceedings of the ASCE Specialty International Conference on The Mexico Earthquakes-1985*, Mexico City, pp 148-162, September.

Romo M. P, Martínez S. A. Flores O. and García S. R. 2010. Diseño geotécnico de la cimentación tipo celda estructurada del apoyo cl-34 del tramo elevado de la Línea 12 del Metro, *Informe del Instituto de Ingeniería a Prefabricados y Transportes S.A. de C.V.* Mayo.

Seed H.B. and Idriss. I.M. 1970. Soil modulus and damping factors for dynamic response analyses, *Report EERC 70-10, EERC,* University of California, Berkeley.

Seed H., Idriss, I. and Arango I. 1981. Evaluation of Liquefaction Potential using Field Performance Data, *ASCE*, Vol. 109, No. 3, pp.458-482.

Vucetic M. and Dobry R. 1991. Effect of soil plasticity on cyclic response, *Journal of Geotech. Engineering,* ASCE, vol. 114, No. 1.